

IMPACT-INDUCED MELTING OF NEAR-SURFACE WATER ICE ON MARS

Sarah T. Stewart^{1,2}, Thomas J. Ahrens¹, and John D. O'Keefe¹

¹*Seismological Laboratory, California Institute of Technology, MC 252-21, Pasadena, CA 91125*

²*Present Address: Dept. Earth & Planetary Sci., Harvard University, 20 Oxford St., Cambridge, MA 02138*

Abstract. All fresh and many older Martian craters with diameters greater than a few km are surrounded by ejecta blankets which appear fluidized, with morphologies believed to form by entrainment of liquid water. We present cratering simulations investigating the outcome of 10 km s^{-1} impacts onto models of the Martian crust, a mixture of basalt and ice at an average temperature of 200 K. Because of the strong impedance mismatch between basalt and ice, the peak shock pressure and the pressure decay profiles are sensitive to the mixture composition of the surface. For typical impact events, about 50% of the excavated ground ice is melted by the impact-induced shock. Pre-existing subsurface liquid water is not required to form observed fluidized ejecta morphologies, and the presence of rampart craters on different age terranes is a useful probe of ground ice on Mars over time.

INTRODUCTION

The ejecta around fresh Martian craters exhibit unusual morphologies compared to ejecta observed on Venus, the Moon and other airless bodies. The dominant characteristic is the appearance of fluidized ground-hugging flow. As early as 1977, after the Viking mission, it was suggested that rampart ejecta resulted from shock-melting of ground ice or excavation of ground water [1]. The presence and complexity of so-called “rampart ejecta,” named after the presence of one or more continuous scarps or “ramparts” around the distal edge of the ejecta blanket, are correlated with crater diameter, D (Fig. 1), latitude, and geologic indicators of ground ice [1-4]. Widespread erosional features on the surface have provided ample evidence that water has existed on the surface of Mars in the past [e.g., 5].

Recent observations by the Gamma Ray Spectrometer on the Mars Odyssey spacecraft support the geologic evidence that ice exists very near the Martian surface in the present day by identifying regions near the poles enriched in hydrogen, which is presumably bound in water [6,

7]. The concentration of hydrogen at the surface is remarkably high and well fit by a layer containing $35 \pm 15\%$ ice by weight (40-73% by volume) beneath a dusty layer 0.1- to 1-m thick [7].

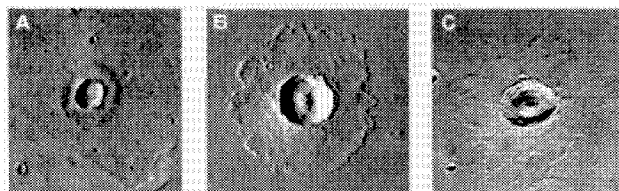


FIGURE 1. Type examples of rampart ejecta morphologies on Mars. A. $D=7.7 \text{ km}$ single pancake ejecta layer around crater (Viking image #608A29). B. $D=15.6 \text{ km}$ single ejecta layer terminating in a rampart (#545A45). C. $D=33.9 \text{ km}$ with multiple layers of ejecta producing a complex rampart crater (#827A01).

The Mars Odyssey measurements are only sensitive to the upper 1 meter, however, and the geologic features indicate that larger quantities of water must have existed at greater depths. Fluidized ejecta features are primarily found around craters with diameters between about 2 and 30 km and ejecta around larger craters are similar to ejecta on dry surfaces [4], implying water-rich

layers in the upper ~2 kilometers. Excavated material from Martian rampart craters reflects the ice content over this depth range. To understand the amount of liquid water that was present in Martian ejecta blankets, we conducted simulations of impact cratering onto ice-rock mixtures using the shock physics code CTH [8] and calculated the volume of ground ice subject to shock-induced melting and the amount of excavated liquid water.

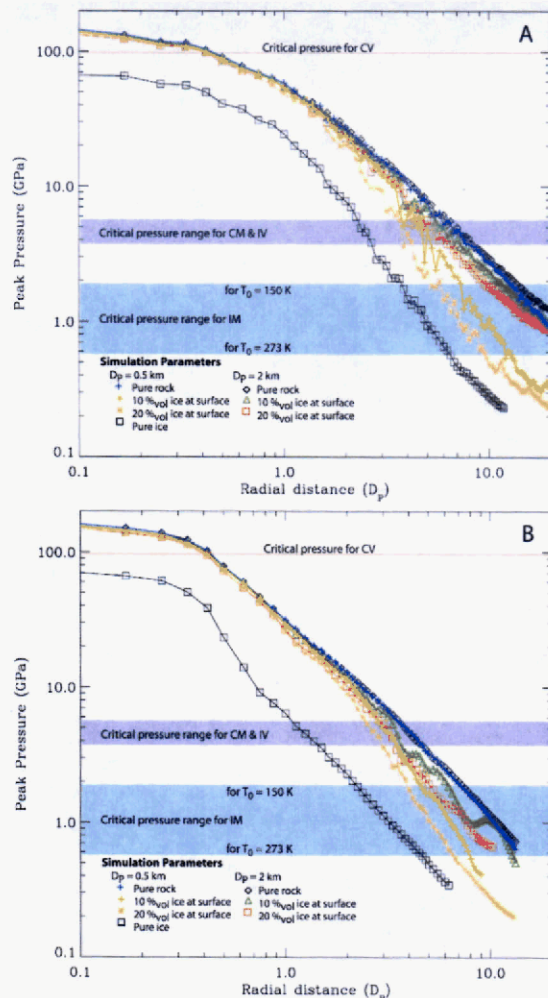


FIGURE 2. Peak shock pressure decay profiles at (A) 45° and (B) 15° from the horizontal. Profiles calculated for 10 km s⁻¹ normal impact by solid rock projectile for annotated ground ice compositions and projectile diameters. Pure ice target provides a lower limit pressure profile. Critical shock pressures for incipient (IM) and complete (CM) melting and vaporization (IV, CV) are shown for initial temperatures between 150 and 273 K.

METHOD

The CTH mesh was initialized with a pure CO₂ atmosphere overlying a silicate crust in gravitational equilibrium. Ground ice is assumed to be distributed within pore spaces and cracks in the Martian regolith at the average surface temperature, 200 K. The atmosphere was approximated as an isothermal ideal gas at 170 K and initialized with the present day mean base pressure of 7 millibar.

The regolith pore space is modeled by assuming pore volume, ϕ , decreases with depth, z , as $\phi = \phi_0 e^{-z/K_z}$, where ϕ_0 is the surface porosity and K_z is the decay constant, estimated to be 3 km [3, 9]. The surface porosity is varied from 0-20% and the ground ice is assumed to fill all available pore space. Each cell in the mesh is initialized with the appropriate mixture of ice and silicate, so that mixed cell thermodynamics is employed from the beginning of the calculation. The ANEOS equation of state [10] for H₂O [11] and dunite are used. The criteria for shock-induced melting of H₂O ice are taken from experimental results [12] and agree well with the ANEOS model.

The two-dimensional cylindrically symmetric simulation begins with the silicate projectile entering the top of the atmosphere at the average asteroidal impactor speed on Mars, 10 km s⁻¹. The dynamic strength of the Martian surface is constrained to ~10 MPa by the observed transition diameter from simple to complex craters on Mars, ~7 km [13]. We varied the projectile diameter (100 to 2000 m) to simulate simple and complex type crater formation.

RESULTS

The range of shock pressures for shock-induced melting of ground ice is summarized in Fig. 2. We display the peak pressure vs. Lagrangian range from impacts with different diameter projectiles (D_p) and ground ice compositions (ϕ_0) at 45° and 15° from the horizontal. The shock front is approximately hemispherical, but near the free surface, the pressure contours decrease more rapidly with

distance from the impact point (Fig. 3A). The 15° profile cuts through the excavated region and the 45° pressure decay profile is similar to the 90° profile.

Ice in the Martian crust, at temperatures between 150 and 273 K, will begin to melt after

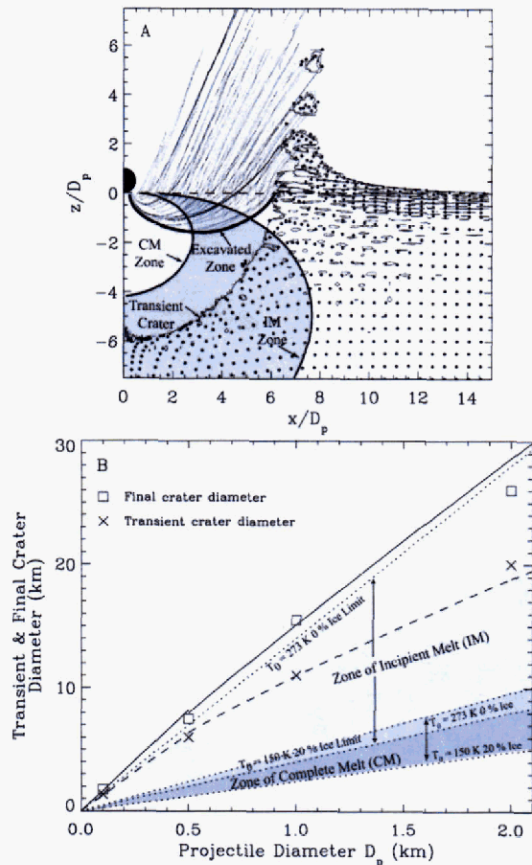


FIGURE 3. Excavation zone and scaling laws for crater diameter, zones of incipient (IM) and complete (CM) melting. A. Crater excavation zone for 500-m diameter projectile impacting at 10 km s^{-1} onto a surface with $\phi_0 = 0.2$. Axes scaled by projectile diameter D_p . Trajectory histories shown for Lagrangian tracer particles (\bullet) at 20 sec. B. Transient (\times , dashed line) and final (\square , solid line) crater diameter as a function of projectile diameter for typical asteroid-derived impactors on Mars. Diameters of zones of partial melting of ground ice and complete melting within the excavated region shown for initial temperatures between 150 K (polar region) and 273 K (equatorial region) and ϕ_0 between 0.0 and 0.2. Solid and dashed lines correspond to crater scaling functions in competent rock [14].

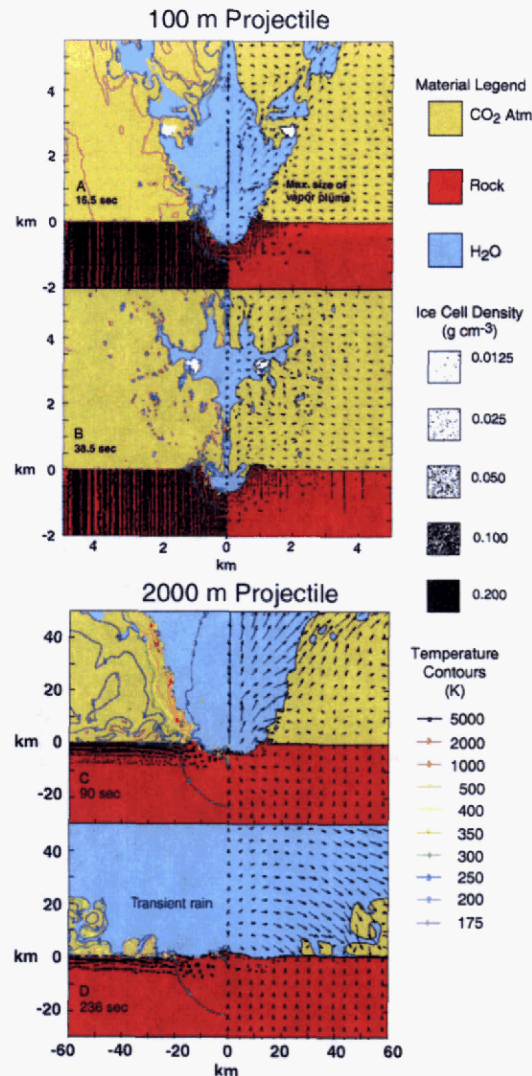


FIGURE 4. Impact cratering time sequences. A-B. Time sequence for 100-m diameter projectile impact onto regolith with 20% vol. near-surface ice. Maximum extent of vapor plume is contained by atmosphere above crater cavity and has no ejecta curtain interaction. C-D. 2000-m diameter projectile. Water vapor plume disrupts regional atmosphere and collapses as transient rain as the water vapor cools and condenses upon adiabatic expansion. Each panel shows ice content (left, shading), temperature contours (left), flow field velocities (right), and major material composition (solid colors). Note calculation mesh is larger than area plotted here.

experiencing shock pressures between 2.0 and 0.6 GPa, respectively, and will completely melt upon

release from shock pressures above 5.5 and 3.7 GPa [12]. Because shock energy is partitioned into melting the ice, the peak pressure decay is steeper in ice-rock mixtures. The effect of ground ice on shock pressure is more pronounced when the projectile size is smaller than the inherent length scale of ice distribution in the crust (K_z). The steepest pressure decay occurs in the ice-rich surfaces between 3 and 6 GPa, around the critical pressure for complete melting. Below the critical shock pressure for incipient melting of ice (0.6 GPa), the decay constant (-1.44) is similar to that from impact events in pure rock (-1.47), which does not undergo widespread melting.

The diameter of the crater at the time of maximum penetration, the transient crater diameter (dashed line, Fig. 3B), is comparable to the final crater diameter (solid line, Fig. 3B) for small, simple craters, but is much less than the final crater diameter for large, complex craters. The diameter of the excavated region is equal to the transient crater diameter, but the depth of excavation is much shallower (Fig. 3A). Ground ice in the inner region of the excavated zone completely melts, whereas less ice is melted in the outer region.

In the present climate, we find that about half the excavated ice is melted by the impact shock. In the equatorial zone, about 60% of the excavated ground ice is completely melted by the impact shock. At the poles, more than 20% is melted. Because of the larger volume, liquid water from the partial melt zone accounts for about half the liquid in the continuous ejecta blanket. These results verify the hypothesis that shock-melting of ground ice will introduce large quantities of liquid water into the ejecta blanket. Therefore, ejecta fluidization does not require pre-existing liquid water near the surface.

Fig. 4 displays time sequences for two diameter impactors, showing the development of the water vapor plume and the interaction of the plume with the ejecta curtain. For craters larger than about 7 km, the vapor plume is massive enough to disrupt the ballistic trajectories of the ejecta.

CONCLUSIONS

Detailed simulations of impact cratering on Mars quantify the effect of ground ice on shock

pressure decay profiles and provide insight into late time processes, such as ejecta emplacement. Using excavation regions from simulations and the critical shock pressures for melting ice, we calculate the amount of liquid water in the ejecta blankets. About half the ground ice in the excavation zone is melted by the impact shock, producing up to meters of liquid water in a single ejecta blanket. Ejecta may be mobilized by entrained liquid water, forming distinct morphologies related to the size of the crater and the amount of ground ice.

ACKNOWLEDGMENTS

This work is supported by NASA. Editorial suggestions proffered by M.D. Furnish are gratefully acknowledged. Contribution #8979, Division of Geological and Planetary Sciences, California Institute of Technology.

REFERENCES

1. Carr, M. H., et al., *J. Geophys. Res.* **82**, 4055-4065 (1977).
2. Kuz'min, R. O., et al., *Solar System Res.* **22**, 121-133 (1988).
3. Squyres, S. W., et al., *Mars*, edited by H.H. Kieffer, et al., U. Arizona, Tucson, 1992, pp. 523-554.
4. Barlow, N. G., *Icarus* **75**, 285-305 (1988).
5. Carr, M. H., *Water on Mars*, Oxford U. P., New York, 1996.
6. Feldman, W. C., et al., *Science* **297**, 75-78 (2002).
7. Boynton, W. V., et al., *Science* **297**, 81-85 (2002).
8. McGlaun, J. M., S. L. Thompson, and M. G. Elrick, *Int. J. Impact Eng.* **10**, 351-360 (1990).
9. Clifford, S. M., *Lunar and Planetary Science Institute Contribution* **441**, 46-48 (1981).
10. Thompson, S. L. and H. S. Lauson, Sandia Laboratories, SC-RR-71 0714, Albuquerque, NM, March, 1972.
11. Turtle, E. P. and E. Pierazzo, *Science* **294**, 1326-1328 (2001).
12. Stewart, S. T. and T. J. Ahrens, *Geophys. Res. Lett.* **30**, 1332, doi: 10.1029/2002GL016789 (2003).
13. Garvin, J. B. and J. J. Frawley, *Geophys. Res. Lett.* **25**, 4405-4408 (1998).
14. Melosh, H. J., *Impact Cratering: A Geologic Process*, Oxford U.P., New York, 1989.